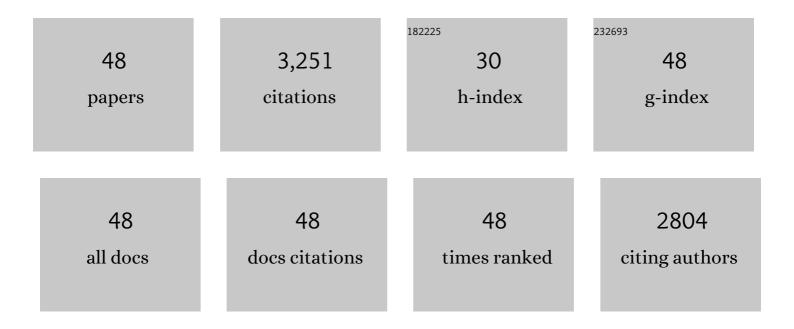
## Yong Feng

List of Publications by Year in descending order

Source: https://exaly.com/author-pdf/8116753/publications.pdf Version: 2024-02-01



YONG FENC

#	Article	IF	CITATIONS
1	Facile pathway towards crystallinity adjustment and performance enhancement of copper selenide for vapor-phase elemental mercury sequestration. Chemical Engineering Journal, 2022, 430, 132811.	6.6	5
2	Favorably adjusting the pore characteristics of copper sulfide by template regulation for vapor-phase elemental mercury immobilization. Journal of Materials Chemistry A, 2022, 10, 10729-10737.	5.2	17
3	Enhanced peroxydisulfate oxidation via Cu(III) species with a Cu-MOF-derived Cu nanoparticle and 3D graphene network. Journal of Hazardous Materials, 2021, 403, 123691.	6.5	38
4	Enhanced Photo–Fenton Removal Efficiency with Core-Shell Magnetic Resin Catalyst for Textile Dyeing Wastewater Treatment. Water (Switzerland), 2021, 13, 968.	1.2	13
5	Advances in flue gas mercury abatement by mineral chalcogenides. Chemical Engineering Journal, 2021, 411, 128608.	6.6	51
6	Facile preparation of nanosized copper sulfide functionalized macroporous skeleton for efficient vapor-phase mercury sequestration. Chemical Engineering Journal, 2021, 419, 129561.	6.6	33
7	Activation of peroxymonosulfate by molybdenum disulfide-mediated traces of Fe(III) for sulfadiazine degradation. Chemosphere, 2021, 283, 131212.	4.2	19
8	Activation of dissolved molecular oxygen by ascorbic acid-mediated circulation of copper(II): Applications and limitations. Separation and Purification Technology, 2021, 275, 119186.	3.9	7
9	Performance and mechanism in degradation of typical antibiotics and antibiotic resistance genes by magnetic resin-mediated UV-Fenton process. Ecotoxicology and Environmental Safety, 2021, 227, 112908.	2.9	26
10	Enhanced mineralization of oxalate by highly active and Stable Ce(III)-Doped g-C3N4 catalyzed ozonation. Chemosphere, 2020, 239, 124612.	4.2	50
11	Nonradical degradation of microorganic pollutants by magnetic N-doped graphitic carbon: A complement to the unactivated peroxymonosulfate. Chemical Engineering Journal, 2020, 392, 123724.	6.6	28
12	Toward an Understanding of Fundamentals Governing the Elemental Mercury Sequestration by Metal Chalcogenides. Environmental Science & Technology, 2020, 54, 9672-9680.	4.6	27
13	Unraveling the Overlooked Involvement of High-Valent Cobalt-Oxo Species Generated from the Cobalt(II)-Activated Peroxymonosulfate Process. Environmental Science & Technology, 2020, 54, 16231-16239.	4.6	310
14	Advances in magnetically recyclable remediators for elemental mercury degradation in coal combustion flue gas. Journal of Materials Chemistry A, 2020, 8, 18624-18650.	5.2	10
15	Development of selenized magnetite (Fe3O4â^'xSey) as an efficient and recyclable trap for elemental mercury sequestration from coal combustion flue gas. Chemical Engineering Journal, 2020, 394, 125022.	6.6	47
16	Amorphous molybdenum selenide intercalated magnetite as a recyclable trap for the effective sequestration of elemental mercury. Journal of Materials Chemistry A, 2020, 8, 14955-14965.	5.2	30
17	Sulfate radical-induced destruction of emerging contaminants using traces of cobalt ions as catalysts. Chemosphere, 2020, 256, 127061.	4.2	23
18	Enhanced mineralization of dimethyl phthalate by heterogeneous ozonation over nanostructured Cu-Fe-O surfaces: Synergistic effect and radical chain reactions. Separation and Purification Technology, 2019, 209, 588-597.	3.9	55

Yong Feng

#	Article	IF	CITATIONS
19	Amorphous Molybdenum Selenide Nanosheet as an Efficient Trap for the Permanent Sequestration of Vaporâ€Phase Elemental Mercury. Advanced Science, 2019, 6, 1901410.	5.6	57
20	One-step tailoring surface roughness and surface chemistry to prepare superhydrophobic polyvinylidene fluoride (PVDF) membranes for enhanced membrane distillation performances. Journal of Colloid and Interface Science, 2019, 553, 99-107.	5.0	66
21	Ultrasound assisted zero valent iron corrosion for peroxymonosulfate activation for Rhodamine-B degradation. Chemosphere, 2019, 228, 412-417.	4.2	114
22	Role of Sulfur Trioxide (SO <sub>3</sub> ) in Gas-Phase Elemental Mercury Immobilization by Mineral Sulfide. Environmental Science & Technology, 2019, 53, 3250-3257.	4.6	58
23	Nanosized Copper Selenide Functionalized Zeolitic Imidazolate Frameworkâ€8 (CuSe/ZIFâ€8) for Efficient Immobilization of Gasâ€Phase Elemental Mercury. Advanced Functional Materials, 2019, 29, 1807191.	7.8	74
24	Cu(II)-enhanced activation of molecular oxygen using Fe(II): Factors affecting the yield of oxidants. Chemosphere, 2019, 221, 383-391.	4.2	8
25	Solvent-free hydrothermal synthesis of gamma-aluminum oxide nanoparticles with selective adsorption of Congo red. Journal of Colloid and Interface Science, 2019, 536, 180-188.	5.0	56
26	Factors and mechanisms that influence the reactivity of trivalent copper: A novel oxidant for selective degradation of antibiotics. Water Research, 2019, 149, 1-8.	5.3	64
27	Highly efficient degradation of dimethyl phthalate from Cu(II) and dimethyl phthalate wastewater by EDTA enhanced ozonation: Performance, intermediates and mechanism. Journal of Hazardous Materials, 2019, 366, 378-385.	6.5	33
28	Activation of persulfate with metal–organic framework-derived nitrogen-doped porous Co@C nanoboxes for highly efficient p-Chloroaniline removal. Chemical Engineering Journal, 2019, 358, 408-418.	6.6	177
29	Enhanced As(III) Sequestration Using Sulfide-Modified Nano-Scale Zero-Valent Iron with a Characteristic Core–Shell Structure: Sulfidation and As Distribution. ACS Sustainable Chemistry and Engineering, 2018, 6, 3039-3048.	3.2	85
30	Activation of Persulfates Using Siderite as a Source of Ferrous Ions: Sulfate Radical Production, Stoichiometric Efficiency, and Implications. ACS Sustainable Chemistry and Engineering, 2018, 6, 3624-3631.	3.2	67
31	Degradation of 1,4-dioxane via controlled generation of radicals by pyrite-activated oxidants: Synergistic effects, role of disulfides, and activation sites. Chemical Engineering Journal, 2018, 336, 416-426.	6.6	77
32	Facile synthesis of highly reactive and stable Fe-doped g-C3N4 composites for peroxymonosulfate activation: A novel nonradical oxidation process. Journal of Hazardous Materials, 2018, 354, 63-71.	6.5	154
33	Cu <sub>2</sub> O-promoted degradation of sulfamethoxazole by <i>α</i> -Fe <sub>2</sub> O <sub>3</sub> -catalyzed peroxymonosulfate under circumneutral conditions: synergistic effect, Cu/Fe ratios, and mechanisms. Environmental Technology (United Kingdom), 2018, 39. 1-11.	1.2	39
34	Immobilization of Lead in Cathode Ray Tube Funnel Glass with Beneficial Use of Red Mud for Potential Application in Ceramic Industry. ACS Sustainable Chemistry and Engineering, 2018, 6, 14213-14220.	3.2	6
35	Dual Roles of Nano-Sulfide in Efficient Removal of Elemental Mercury from Coal Combustion Flue Gas within a Wide Temperature Range. Environmental Science & Technology, 2018, 52, 12926-12933.	4.6	52
36	Phosphorus recovery through adsorption by layered double hydroxide nano-composites and transfer into a struvite-like fertilizer. Water Research, 2018, 145, 721-730.	5.3	87

Yong Feng

#	Article	IF	CITATIONS
37	Supported palladium nanoparticles as highly efficient catalysts for radical production: Support-dependent synergistic effects. Chemosphere, 2018, 207, 27-32.	4.2	9
38	Applicability study on the degradation of acetaminophen via an H2O2/PDS-based advanced oxidation process using pyrite. Chemosphere, 2018, 212, 438-446.	4.2	42
39	Rapid Selective Circumneutral Degradation of Phenolic Pollutants Using Peroxymonosulfate–Iodide Metal-Free Oxidation: Role of Iodine Atoms. Environmental Science & Technology, 2017, 51, 2312-2320.	4.6	86
40	Mini‣ized Carbon Nitride Nanosheets with Double Excitation―and pHâ€Dependent Fluorescence Behaviors for Twoâ€Photon Cell Imaging. Chemistry - an Asian Journal, 2017, 12, 835-840.	1.7	5
41	Degradation of contaminants by Cu + -activated molecular oxygen in aqueous solutions: Evidence for cupryl species (Cu 3+ ). Journal of Hazardous Materials, 2017, 331, 81-87.	6.5	99
42	Surface-bound sulfate radical-dominated degradation of 1,4-dioxane by alumina-supported palladium (Pd/Al 2 O 3 ) catalyzed peroxymonosulfate. Water Research, 2017, 120, 12-21.	5.3	172
43	Response to Comment on "Rapid Selective Circumneutral Degradation of Phenolic Pollutants Using Peroxymonosulfate–Iodide Metal-Free Oxidation: Role of Iodine Atoms― Environmental Science & Technology, 2017, 51, 9412-9413.	4.6	4
44	Opposite effects of dissolved oxygen on the removal of As(III) and As(V) by carbonate structural Fe(II). Scientific Reports, 2017, 7, 17015.	1.6	26
45	Effect of Nitrogen Oxides on Elemental Mercury Removal by Nanosized Mineral Sulfide. Environmental Science & Technology, 2017, 51, 8530-8536.	4.6	75
46	Mineralization of perfluorooctanesulfonate (PFOS) and perfluorodecanoate (PFDA) from aqueous solution by porous hexagonal boron nitride: adsorption followed by simultaneous thermal decomposition and regeneration. RSC Advances, 2016, 6, 113773-113780.	1.7	20
47	Copper-promoted circumneutral activation of H2O2 by magnetic CuFe2O4 spinel nanoparticles: Mechanism, stoichiometric efficiency, and pathway of degrading sulfanilamide. Chemosphere, 2016, 154, 573-582.	4.2	87
48	Sulfate Radical-Mediated Degradation of Sulfadiazine by CuFeO <sub>2</sub> Rhombohedral Crystal-Catalyzed Peroxymonosulfate: Synergistic Effects and Mechanisms. Environmental Science & Technology, 2016, 50, 3119-3127.	4.6	563